

Picosecond Phenomena III

Proceedings of the Third International Conference
on Picosecond Phenomena
Garmisch-Partenkirchen, Fed. Rep. of Germany
June 16-18, 1982

Editors

K.B. Eisenthal R.M. Hochstrasser W. Kaiser
A. Laubereau

With 288 Figures

Springer-Verlag Berlin Heidelberg New York 1982

Contents

Part I **Advances in the Generation of Ultrashort Light Pulses**

Moving from the Picosecond to the Femtosecond Time Regime By C.V. Shank, R.L. Fork, and R.T. Yen	2
Femtosecond Optical Pulses: Towards Tunability at the Gigawatt Level By A. Migus, J.L. Martin, R. Astier, A. Antonetti, and A. Orszag ..	6
Femtosecond Continuum Generation. By R.L. Fork, C.V. Shank, R.T. Yen, C. Hirlimann, and W.J. Tomlinson	10
New Picosecond Sources and Techniques By A.E. Siegman and H. Vanherzeele	14
Generation of Coherent Tunable Picosecond Pulses in the XUV By T. Srinivasan, K. Boyer, H. Egger, T.S. Luk, D.F. Muller, H. Pummer, and C.K. Rhodes	19
New Infrared Dyes for Synchronously Pumped Picosecond Lasers By A. Seilmeier, B. Kopainsky, W. Kranitzky, W. Kaiser, and K.H. Drexhage	23
Acousto-Optic Stabilization of Mode-Locked Pulsed Nd:YAG Laser By H.P. Kortz	27
Active Mode Stabilization of Synchronously Pumped Dye Lasers By A.I. Ferguson and R.A. Taylor	31
Spectral Hole Burning in the Saturation Region of Mode-Locked Nd-Glass Lasers. By A. Penzkofer and N. Weinhardt	36
Single and Double Mode-Locked Ring Dye Lasers; Theory and Experiment By K.K. Li, G. Arjavalingam, A. Dienes, and J.R. Whinnery	40
Theoretical and Experimental Investigations of Colliding Pulse Mode-Locking (CPM). By W. Dietel, D. Kühlke, W. Rudolph, and B. Wilhelmi	45
Picosecond Carrier Dynamics and Laser Action in Optically Pumped Buried Heterostructure Lasers By T.L. Koch, L.C. Chiu, Ch. Harder, and A. Yariv	49
Optically Pumped Semiconductor Platelet Lasers in External Cavities By M.M. Salour	53

Two Photon Pumped Bulk Semiconductor Laser for the Generation of Picosecond Pulses. By Wei-Lou Cao, Fei-Ming Tong, De-Sen Shao, S.A. Strobel, V.K. Mathur, and Chi H. Lee	57
The Pulse Duration of a Distributed Feedback Dye Laser Under Single Pulse Conditions. By Z. Bor, B. Răcz, G. Szabó, and A. Müller	62
Picosecond Distributed Feedback Dye Laser Tunable in a Broad Spectral Range. By A.N. Rubinov, I. Chesnulyavichus, and T.Sh. Efendiev	66
Modelocking of a Wavelength Tunable High-Pressure CO ₂ -Laser by Synchronous Modulation of a Broadband Intracavity Saturable Absorber. By J.K. Ajo, Y. Hefetz, and A.V. Nurmikko	68
The Non-Mode-Locked Picosecond Laser By F. Armani, F. DeMartini, and P. Mataloni	71
A Novel Method for Generating Sub-Transform Limited Picosecond Nd:YAG Laser Pulses. By S.C. Hsu and H.S. Kwok	74
Optical Dephasing in Inorganic Glasses By R.M. Shelby and R.M. MacFarlane	78
 <i>Part II Ultrashort Measuring Techniques</i>	
Picosecond Holographic Grating Experiments in Molecular Condensed Phases. By M.D. Fayer	82
Self-Diffraction from Laser-Induced Orientational Gratings in Semiconductors. By A.L. Smirl, T.F. Boggess, B.S. Wherrett, G.P. Perryman, and A. Miller	87
A Picosecond Raman Technique with Resolution Four Times Better than Obtained by Spontaneous Raman Spectroscopy By W. Zinth, M.C. Nuss, and W. Kaiser	91
Broadband CARS Probe Using the Picosecond Continuum By L.S. Goldberg	94
Jitter-Free Streak Camera System By W. Knox, T.M. Nordlund, and G. Mourou	98
Electrical Transient Sampling System with Two Picosecond Resolution By J.A. Valdmanis, G. Mourou, and C.W. Gabel	101
High-Resolution Picosecond Modulation Spectroscopy of Near Interband Resonances in Semiconductors By S. Sugai, J.H. Harris, and A.V. Nurmikko	103
Electron Diffraction in the Picosecond Domain Steven Williamson and Gerhard Mourou and Synchronous Amplification of 70 fsec Pulses Using a Frequency-Doubled Nd:YAG Pumping Source. By J.D. Kafka, T. Sizer II, I.N. Duling, C.W. Gabel, and G. Mourou	107

Picosecond Time-Resolved Photoacoustic Spectroscopy By M. Bernstein, L.J. Rothberg, and K.S. Peters	112
Subpicosecond Pulse Shape Measurement and Modeling of Passively Mode- Locked Dye Lasers Including Saturation and Spatial Hole Burning By J.-C. Diels, I.C. McMichael, J.J. Fontaine, and C.Y. Wang	116
Experimental Demonstration of a New Technique to Measure Ultrashort Dephasing Times By J.C. Diels, W.C. Wang, P. Kumar, and R.K. Jain	120
Optical Pulse Compression with Reduced Wings By D. Grischkowsky and A.C. Balant	123
Polariton-Induced Compensation of Picosecond Pulse Broadening in Optical Fibers. By G.W. Fehrenbach and M.M. Salour	126
 Part III Advances in Optoelectronics	
Generation and Pulsewidth Measurement of Amplified Ultrashort Ultraviolet Laser Pulses in Krypton Fluoride. By P.H. Bucksbaum, J. Bokor, R.H. Storz, J.W. White, and D.H. Auston	130
Addressing and Control of High-Speed GaAs FET Logic Circuits with Picosecond Light Pulses By R.K. Jain, J.E. Brown, and D.E. Snyder	134
Surface Metal-Oxide-Silicon-Oxide-Metal Picosecond Photodetector By S. Thaniyavarn and T.K. Gustafson	137
Solid-State Detector for Single-Photon Measurements of Fluorescence Decays with 100 Picosecond FWHM Resolution By A. Andreoni, S. Cova, R. Cubeddu, and A. Longoni	141
Picosecond Optoelectric Modulation of Millimeter-Waves in GaAs Waveguide By M.G. Li, V.K. Mathur, Wei-Lou Cao, and Chi H. Lee	145
Synchroscan Streak Camera Measurements of Mode-Propagation in Optical Fibers. By J.P. Willson, W. Sibbett, and P.G. May	149
 Part IV Relaxation Phenomena in Molecular Physics	
Picosecond Lifetimes and Efficient Decay Channels of Vibrational Models of Polyatomic Molecules in Liquids By C. Kolmeder, W. Zinth, and W. Kaiser	154
Vibrational Population Decay and Dephasing of Small and Large Polyatomic Molecules in Liquids By H. Graener, D. Reiser, H.R. Telle, and A. Laubereau	159
Mechanisms for Ultrafast Vibrational Energy Relaxation of Polyatomic Molecules. By S.F. Fischer	164

Studies of the Generation and Energy Relaxation in Chemical Intermediates-Divalent Carbon Molecules and Singlet Oxygen By E.V. Sitzmann, C. Dupuy, Y. Wang, and K.B. Eisenthal	168
New Developments in Picosecond Time-Resolved Fluorescence Spectroscopy: Vibrational Relaxation Phenomena By B.P. Boczar and M.R. Topp	174
Picosecond Photon Echo and Coherent Raman Scattering Studies of Dephasing in Mixed Molecular Crystals By K. Duppen, D.P. Weitekamp, and D.A. Wiersma	179
Picosecond Laser Spectroscopy of Molecules in Supersonic Jets: Vibrational Energy Redistribution and Quantum Beats By A.H. Zewail	184
Picosecond Studies of Intramolecular Vibrational Redistribution in S_1 <i>p</i> -Difluorobenzene Vapor. By R.A. Coveleskie, D.A. Dolson, S.C. Muchak , C.S. Parmenter, and B.M. Stone	190
Direct Picosecond Resolving of Hot Luminescence Spectrum By J. Aaviksoo, A. Anijalg, A. Freiberg, M. Lepik, P. Saari, T. Tamm, and K. Timpmann	192
The Temperature Dependence of Homogeneous and Inhomogeneous Vibrational Linewidth Broadening Studies Using Coherent Picosecond Stokes Scattering. By S.M. George, A.L. Harris, M. Berg, and C.B. Harris	196
A Picosecond CARS-Spectrometer Using Two Synchronously Mode-Locked CW Dye Lasers. By J. Kuhl and D. von der Linde	201
Picosecond Studies of Intramolecular Charge Transfer Processes in Excited A-D Molecules By H. Staerk, R. Mitzkus, W. Kühnle, and A. Weller	205
Femtosecond Transient Birefringence in CS_2 By B.I. Greene and R.C. Farrow	209
Time-Resolved Observation of Molecular Dynamics in Liquids by Femtosecond Interferometry. By C.L. Tang and J.M. Halbout	212
Time-Resolved Measurement of Non-linear Susceptibilities by Optical Kerr Effect. By J. Etchepare, G. Grillon, R. Astier, J.L. Martin, C. Bruneau, and A. Antonetti	217
Subpicosecond Laser Spectroscopy: Pulse Diagnostics and Molecular Dynamics in Liquids. By C. Kalpouzos, G.A. Kenney-Wallace, P.M. Kroger, E. Quitevis, and S.C. Wallace	221
Viscosity-Dependent Internal Rotation in Polymethine Dyes Measured by Picosecond Fluorescence Spectroscopy By A.C. Winkworth, A.D. Osborne, and G. Porter	228
Rotational Diffusion in Mixed Solvents Measured by Picosecond Fluorescence Anisotropy. By T. Doust and G.S. Beddard	232

Investigation of Level Kinetics and Reorientation by Means of Double Pulse Excited Fluorescence By D. Schubert, J. Schwarz, H. Wabnitz, and B. Wilhelmi	235
Dynamics of Photoisomerization By G.R. Fleming, S.P. Velsko, and D.H. Waldeck	238
Evidence for the Existence of a Short-Lived Twisted Electronic State in Triphenylmethane Dyes By V. Sundström, T. Gillbro, and H. Bergström	242
Kinetics of Stimulated and Spontaneous Emission of Dye Solutions Under Picosecond Excitation. By B.A. Bushuk, A.N. Rubinov, A.A. Murav'ov, and A.P. Stupak	246
Picosecond Resolution Studies of Ground State Quantum Beats and Rapid Collisional Relaxation Processes in Sodium Vapor By R.K. Jain, H.W.K. Tom, and J.C. Diels	250
 Part V Picosecond Chemical Processes	
Unimolecular Processes and Vibrational Energy Randomization By R.A. Marcus	254
Picosecond Dynamics of I ₂ Photodissociation. By P. Bado, P.H. Berens, J.P. Bergsma, S.B. Wilson, K.R. Wilson, and E.J. Heller	260
Vibrational Predissociation of S-Tetrazine-Ar van der Waals-Molecules By J.J.F. Ramaekers, J. Langelaar, and R.P.H. Rettschnick	264
Picosecond Laser Induced Fluorescence Probing of NO ₂ Photofragments By P.E. Schoen, M.J. Marrone, and L.S. Goldberg	269
Excited State Proton Transfer in 2-(2-'Hydroxyphenyl)-Benzoxazole By G.J. Woolfe, M. Melzig, S. Schneider, and F. Dörr	273
Picosecond Dynamics of Unimolecular Ion Pair Formation By K.G. Spears, T.H. Gray, and D. Huang	278
Effect of Polymerization on the Fluorescence Lifetime of Eosin in Water By Wei-Zhu Lin, Yong-Lian Zhang, and Xin-Dong Fang	282
 Part VI Ultrashort Processes in Biology	
Picosecond Processes Involving CO, O ₂ , and NO Derivatives of Hemeproteins. By P.A. Cornelius and R.M. Hochstrasser	288
Femtosecond and Picosecond Transient Processes After Photolysis of Liganded Hemeproteins. By J.L. Martin, C. Poyart, A. Migus, Y. Lecarpentier, R. Astier, and J.P. Chambaret	294
Picosecond Fluorescence Spectroscopy of Hematoporphyrin Derivative and Related Porphyrins By M. Yamashita, T. Sato, K. Aizawa, and H. Kato	298

Resonance Raman Spectra of Picosecond Transients: Application to Bacteriorhodopsin. By M.A. El-Sayed, Chung-Lu Hsieh, and M. Nicol	302
Picosecond Studies of Bacteriorhodopsin Intermediates from 11-cis Rhodopsin and 9-cis Rhodopsin. By J.-D. Spalink, M.L. Applebury, W. Sperling, A.H. Reynolds, and P.M. Rentzepis	307
Multiple Photon Processes in Molecules Induced by Picosecond UV Laser Pulses. By V.S. Antonov, E.V. Khoroshilova, N.P. Kuzmina, V.S. Letokhov, Yu.A. Matveetz, A.N. Shibanov, and S.E. Yegorov	310
P-BR and Its Role in the Photocycle of Bacteriorhodopsin By T. Gillbro and V. Sundström	315
Picosecond Linear Dichroism Spectroscopy of Retinal. By M.E. Lippitsch, M. Riegler, F.R. Aussenegg, L. Margulies, and Y. Mazur	319
Picosecond Absorption Spectroscopy of Biliverdin By M.E. Lippitsch, M. Riegler, A. Leitner, and F.R. Aussenegg	323
Picosecond Time-Resolved Resonance Raman Spectroscopy of the Photolysis Product of Oxy-Hemoglobin By J. Turner, T.G. Spiro, D.F. Voss, C. Paddock, and R.B. Miles	327
 Part VII Applications in Solid-State Physics	
Picosecond Time-Resolved Detection of Plasma Formation and Phase Transition in Silicon By J.M. Liu, H. Kurz, and N. Bloembergen	332
Spectroscopy of Picosecond Relaxation Processes in Semiconductors By D. von der Linde, N. Fabricius, J. Kuhl, and E. Rosengart	336
Picosecond Spectroscopy of Excitonic Molecules and High Density Electron-Hole Plasma in Direct-Gap Semiconductors. By S. Shionoya	341
Picosecond Time-Resolved Study of Highly Excited CuCl. By D. Hulin, A. Antonetti, L.L. Chase, G. Hamoniaux, A. Migus, and A. Mysyrowicz	345
Picosecond Dynamics of Excitonic Polariton in CuCl By Y. Aoyagi, Y. Segawa, and S. Namba	349
Picosecond Spectroscopy of Highly Excited GaAs and CdS By H. Saito, W. Graudszus, and E.O. Göbel	353
Non-Linear Attenuation of Excitonic Polariton Pulses in CdSe By P. Lavallard and P.H. Duong	357
Time-Resolved Photoluminescence Study of n Type CdS and CdSe Photoelectrode By D. Huppert, Z. Harzion, N. Croitoru, and S. Gottesfeld	360
Time-Resolved Spatial Expansion of the Electron-Hole Plasma in Polar Semiconductors By A. Cornet, T. Amand, M. Pagnet, and M. Brousseau	364

Weak-Wave Retardation and Phase-Conjugate Self-Defocusing in Si By E.W. Van Stryland, A.L. Smirl, T.F. Boggess, and F.A. Hopf	368
Ultrafast Relaxations of Photoinduced Carriers in Amorphous Semiconductors. By Z. Vardeny, J. Strait, and J. Tauc	372
Periodic Ripple Structures on Semiconductors Under Picosecond Pulse Illumination. By P.M. Fauchet, Zhou Guosheng, and A.E. Siegman	376
Transmission of Picosecond Laser-Excited Germanium at Various Wavelengths. By C.Y. Leung and T.W. Nee	380
Nonlinear Interactions in Indium Antimonide By M. Hasselbeck and H.S. Kwok	384
Picosecond Relaxation Kinetics of Highly Photogenerated Carriers in Semiconductors By S.S. Yao, M.R. Junnarkar, and R.R. Alfano	389
Picosecond Radiative and Nonradiative Recombination in Amorphous As ₂ S ₃ By T.E. Orłowski, B.A. Weinstein, W.H. Knox, T.M. Nordlung, and G. Mourou	395
<i>Index of Contributors</i>	399

Picosecond Lifetimes and Efficient Decay Channels of Vibrational Models of Polyatomic Molecules in Liquids

C. Kolmeder, W. Zinth, and W. Kaiser

Physik Department der Technischen Universität München,
D-8000 München, Fed. Rep. of Germany

Convincing evidence is presented that anharmonic coupling between fundamental vibrational modes and overtones or combination modes is of major importance for the lifetime of vibrational states. The selection rules known to hold for Fermi resonance determine the decay channels. In a number of examples the decay pathways of vibrational energy were observed experimentally by measuring the population and depopulation of subsequent vibrations. Drastic variations of vibrational lifetimes were found for different vibrations of the same molecule.

Molecules are first excited by an ultrashort resonant infrared pulse and the instantaneous degree of excitation is monitored by observing the anti-Stokes Raman signal of a delayed probe pulse. Different vibrational modes are distinguished by their characteristic anti-Stokes frequency.

We have investigated numerous molecules and found widely varying values of the population life-times between 1 ps and 240 ps in polyatomic molecules at room temperature /1,2/. Special attention was paid to the CH-stretching modes in the frequency range of $3000 \pm 100 \text{ cm}^{-1}$.

Vibrational energy is transferred from the CH-stretching modes ($\sim 3000 \text{ cm}^{-1}$) via overtones and combination modes to lower energy states. Intramolecular anharmonic coupling, the Fermi resonance, manifests itself in the infrared and Raman spectra. Overtones and higher order combination modes borrow intensity from CH-stretching modes. We define as a measure of Fermi-resonance mixing the intensity ratio, R , between the final and initial state taken from the infrared or Raman spectrum. In a recent publication a formula was derived which allows to estimate the life time T_1 of vibrational states:

$$T_1 = N(1-R)^2 R^{-1} \exp(\omega/\Omega)^{2/3} T_2(f) \quad (1)$$

N corresponds to the number of states initially excited, R is a measure of the Fermi resonance, and $T_2(f)$ stands for the dephasing time of the final state. $T_2(f)$ may be estimated from the Raman line-width $\Delta\tilde{\nu}$ as $T_2(f) = (2\pi c \Delta\tilde{\nu})^{-1}$ ($T_2(f)$ is equal to $T_2/2$ measured in coherent Raman experiments). The frequency ω represents the energy difference between the initial and final state. Ω has a value close to 100 cm^{-1} .

As an example for the importance of Fermi resonance we present data of the two molecules 1,1-dichloroethene and trans 1,2-

dichloroethene which are made up of the same atoms; only two atoms have exchanged their positions. The infrared and Raman spectra between 2950 cm^{-1} and 3250 cm^{-1} of both molecules are depicted in Fig.1. There are drastic differences in the anharmonic coupling of the CH-stretching modes. In Fig.1a we see strong Fermi resonance of $\text{CH}_2=\text{CCl}_2$ between the fundamental ν_1 and $\nu_2+\nu_3$, both of A_1 symmetry and between the fundamental ν_7 and $\nu_2+\nu_6+\nu_{11}$, both of B_1 symmetry /3/. This observation suggests that we have to consider at least two decay channels for the CH_2 -stretching modes. For the decay $\nu_1 \rightarrow \nu_2+\nu_3$ we estimate the intensity ratio $R = 0.2 \pm 0.05$ and calculate $T_2(f) = 0.3$ ps from the Raman line-width of $\Delta\tilde{\nu} = 17$ cm^{-1} . With $N=1$ and $\omega = 45$ cm^{-1} we calculate from (1) a value of $T_1 = 4 \pm 2$ ps. For the second decay channel $\nu_7 \rightarrow \nu_2+\nu_6+\nu_{11}$ we have to take a short dephasing time $T_2(f)$ of the combination mode. We estimate $T_2(\nu_2+\nu_6+\nu_{11}) \approx 0.2$ ps from the observed line width. With $R = 0.6 \pm 0.1$, $N=1$ and $\omega = 45$ cm^{-1} we calculate $T_1 = 1.5$ ps.

According to Figs.1a and 1b the symmetric (ν_1) and asymmetric (ν_7) CH_2 -stretching vibrations are separated by 100 cm^{-1} . We estimate an energy-transfer time between the CH_2 -stretching modes of $T_1(\nu_1 \rightarrow \nu_7) \approx 3.3$ ps using the formula $T_1(\omega_1 \rightarrow \omega_7) = T_2(\omega_1) \exp(\omega/\Omega)^{2/3}$, where $T_2(\omega_1)$ was taken from the Raman spectrum.

The estimates given here indicate that vibrational energy flows faster out of the ν_7 mode than it is supplied by the transfer $\nu_1 \rightarrow \nu_7$. For the excited and interrogated mode ν_1 we simply add the two decay rates for the two decay channels $\nu_1 \rightarrow \nu_7$ and $\nu_1 \rightarrow \nu_2+\nu_3$ and arrive at a lifetime $T_1(\nu_1) \approx 2$ ps.

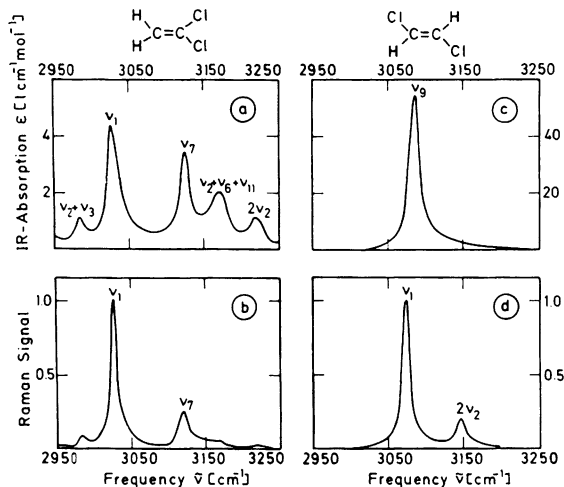


Fig.1 Infrared absorption (a) and Raman (b) spectra of CH_2CCl_2 between 2950 and 3250 cm^{-1} . Two combination tones are in strong Fermi resonance with the two CH-stretching modes ν_1 and ν_7 . Infrared absorption (c) and Raman (d) spectra of trans-CHClCHCl . There is less Fermi-resonance mixing than in CH_2CCl_2 .

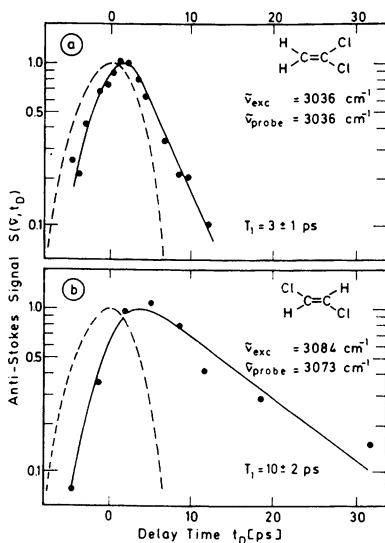


Fig.2 Anti-Stokes scattering signal versus delay time of the probing pulse. (a) CH_2CCl_2 in CCl_4 ($c = 0.35$ m.f.). The decay of the CH_2 -stretching mode at 3036 cm^{-1} is shown. (b) trans CHClCHCl in CCl_4 ($c = 0.35$ m.f.). The CH -stretching mode at 3084 cm^{-1} is excited and the mode at 3073 cm^{-1} is monitored. The broken curves are the cross-correlation functions of the IR exciting and green probing pulses.

In Fig.2a we present experimental data of the direct determination of the T_1 value. The scattered Raman signal of the ν_1 mode rises to a slightly delayed maximum during the excitation process and decays with a relaxation time of T_1 discussed in the preceding paragraph. The broken curves in Fig.2 are cross-correlation curves of the excitation and probing pulse; they determine the zero point on the time axis and give a good indication of the time resolution of the experiment.

In Fig.1c we see the infrared active CH -stretching mode ν_9 and in Fig.1d the Raman active symmetric ν_1 mode of trans CHClCHCl . Here we find a considerably smaller Fermi resonance. The Raman spectrum of Fig.1d suggests some anharmonic coupling between ν_1 and $2\nu_2$, both of A_g symmetry $/3/$. With the values $R = 0.15 \pm 0.02$, $T_2 = 0.3\text{ ps}$, $N=2$ and $\omega = 80\text{ cm}^{-1}$ we calculate $T_1 = 13\text{ ps}$. It should be noted that there might be additional weak Fermi resonance between the ν_9 mode and higher combination modes (e.g. $\nu_2 + \nu_5 + \nu_{10}$) buried under the high frequency tail of the ν_9 fundamental. These additional decay channels may reduce somewhat the estimated T_1 value.

The time dependence of the CH -stretching modes of trans CHClCHCl is depicted in Fig.2b. The molecule is excited via the ν_9 mode at 3084 cm^{-1} and the population of the ν_1 mode at 3073 cm^{-1} is monitored by anti-Stokes Raman scattering. The rapid rise of the Raman signal, i.e. the fast population of the ν_1 mode, gives

clear evidence of the quick energy exchange between the two CH fundamentals ν_1 and ν_9 . The decay of the signal curve suggests a long lifetime of the two CH-stretching modes of $T_1 = 10 \pm 2$ ps. This number is in good agreement with the value estimated above. The small intramolecular coupling gives rise to the longer vibrational life time.

The vibrational states of acetylene are well documented in the literature /4/. Inspection of the energy-level system (see Fig.3) suggests the following interesting situations:(i) Energy in the high lying CH-stretching modes around 3200 cm^{-1} readily flows into several combination modes, all of which comprise the symmetric C \equiv C-stretching mode at $\nu_2 = 1968 \text{ cm}^{-1}$. (ii) The energy transfer from the ν_2 mode to neighboring combination modes is forbidden by symmetry selection rules. Thus we expect a long population life-time of the ν_2 mode.

Experimentally we investigated a solution of C_2H_2 in CCl_4 . Acetylene molecules first are vibrationally excited via the infrared active CH-stretching mode $\nu_3 = 3287 \text{ cm}^{-1}$ and the population and depopulation of the ν_2 mode at 1968 cm^{-1} is monitored. In Fig.4 we indeed see a rapid population of the ν_2 mode within ≤ 3 ps and a very slow depopulation with a time constant of 240 ps. The ν_2 mode in acetylene represents a bottle-neck state. It exhibits the longest relaxation time observed so far in a polyatomic molecule in the liquid state at room temperature.

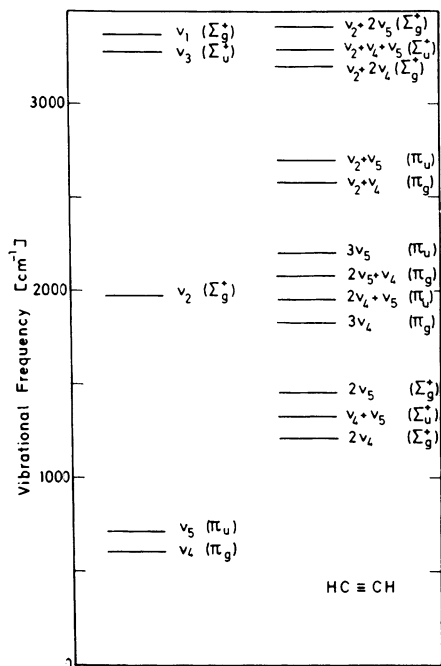


Fig.3 Energy-level diagram of Acetylene

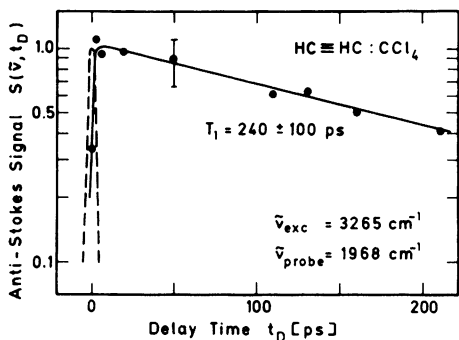


Fig. 4 Anti-Stokes scattering signal of C_2H_2 in CCl_4 versus delay time. Excitation frequency is 3265 cm^{-1} . The decay of the $C\equiv C$ mode at 1968 cm^{-1} is monitored.

References

- 1 A. Fendt, S.F. Fischer, and W. Kaiser, *Chem. Phys.* **57**, 55 (1981)
- 2 A. Fendt, S.F. Fischer, and W. Kaiser, *Chem. Phys. Lett.* **82**, 350 (1981)
- 3 L.M. Sverdlov, M.A. Kovner, E.P. Krainov, *Vibrational Spectra of Polyatomic Molecules*, Wiley, New York, N.Y. 1974, and references therein
- 4 G. Herzberg, *Infrared and Raman spectra of Polyatomic Molecules* von Nostrand, Princeton, N.J. 1945